

## Ibrahim M. Mohamed<sup>1</sup>

Head of Subsurface Engineering Team  
Advantek Waste Management Services,  
Houston, TX 77042  
e-mail: imohamed@advantekwms.com

## Gareth I. Block

Chief Operating Officer  
Advantek Waste Management Services,  
Houston, TX 77042  
e-mail: Gareth@advantekwms.com

## Omar A. Abou-Sayed

Chief Executive Officer  
Advantek Waste Management Services,  
Houston, TX 77042  
e-mail: Omar@advantekwms.com

## Salaheldin M. Elkhatny<sup>2</sup>

Advantek International,  
Houston, TX 77042  
e-mail: elkhatny@kfupm.edu.sa

## Ahmed S. Abou-Sayed

Founder  
Advantek Waste Management Services,  
Houston, TX 77042  
e-mail: ASA@advantekwms.com

# Flow Rate-Dependent Skin in Water Disposal Injection Well

*Reinjection is one of the most important methods to dispose fluid associated with oil and natural gas production. Disposed fluids include produced water, hydraulic fracture flow back fluids, and drilling mud fluids. Several formation damage mechanisms are associated with the injection including damage due to filter cake formed at the formation face, bacteria activity, fluid incompatibility, free gas content, and clay activation. Fractured injection is typically preferred over matrix injection because a hydraulic fracture will enhance the well injectivity and extend the well life. In a given formation, the fracture dimensions change with different injection flow rates due to the change in injection pressures. Also, for a given flow rate, the skin factor varies with time due to the fracture propagation. In this study, well test and injection history data of a class II disposal well in south Texas were used to develop an equation that correlates the skin factor to the injection flow rate and injection time. The results show that the skin factor decreases with time logarithmically as the fracture propagates. At higher injection flow rates, the skin factor achieved is lower due to the larger fracture dimensions that are developed at higher injection flow rates. The equations developed in this study can be applied for any water injector after calibrating the required coefficients using injection step rate test (SRT) data. [DOI: 10.1115/1.4033400]*

## 1 Introduction

Produced water is a by-product of oil and gas production. The produced water can include formation water, injected water, condensed water, and trace amounts of treatment chemicals [1–2]. It is the largest volume by-product or waste stream associated with oil and gas exploration and production, estimated at  $21 \times 10^9$  barrels per year ( $57.4 \times 10^6$  bbl/day) in the United States in 2007 [3]. The estimated water oil ratio worldwide is 2:1 to 3:1. In the U.S., this ratio reached as high as 8:1 because many U.S. fields were mature and past their peak production. The ratio may be even higher, as many older U.S. wells have ratios  $>50:1$  [4].

In the U.S., 98% of the water produced from onshore wells is injected into underground formations. Fifty-nine percent is used in waterflooding to support the oil reservoir pressure and increase oil production, and 40% is disposed into nonproducing formations. The remaining 2% was managed through surface disposal including evaporation ponds, offsite commercial disposal, beneficial reuse, and other management methods. While more than 91% of the water produced from the offshore wells is discharged to the ocean, most of the remaining volume is injected for enhanced oil recovery (EOR) purposes [4].

Underground water injection and disposal are performed through class II wells. Class II wells are the wells that inject fluids for EOR, dispose of fluids associated with oil and gas production, and inject liquid hydrocarbon for storage. (Of approximately 144,000 class II wells in the U.S., salt water disposal represents 20%.) [5]

Besides produced water, oil field waste waters are a mixture of many different streams, including cooling tower blowdown, boiler water blowdown, ion exchange bed regeneration stream, filter backwash, cleaning solutions (acids, caustic, and detergents), and corrosion inhibitors and biocides.

**1.1 Formation Damage During Water Injection.** Water quality is the most important factor that affects the formation during water injection. Water quality refers to the chemical, physical, and biological characteristics of water [6]. Five components in water detrimental to water injection include microorganisms, dispersed oil, suspended solids, dissolved gases, and dissolved solids [7].

A formation can be subjected to several mechanisms by the injection of low quality water, which cause damage (i.e., reduction of the formation permeability) including mechanical damage due to injection of solids or fines migration [8]; interaction between the formation minerals and injected water that might cause clay activation (swelling and/or deflocculation) [9], formation dissolution, chemical adsorption and wettability alternation, relative permeability alterations due to multiphase flow, biological damage due to the presence of bacteria [10]; interaction between formation brine and incompatible injected water that can produce insoluble scales, emulsions, wax, and asphaltene deposition [11]; and non-Darcy flow effects [12]. Oily water waste may also become adsorbed inside the formation and block the pore throats, although this effect is more pronounced in water-wet than in oil-wet formations [13]. Modeling fracture damage can help in predicting more accurately the decline in the production flow rate from a propped fracture well [14].

The mitigation technique to avoid loss of the formation injectivity depends on the formation damage mechanism. Water filtration is essential to avoid mechanical damage by removing solid particles larger than 10% of the pore diameter. Using clay inhibitor is a must in clay-rich formations to prohibit clay swelling

<sup>1</sup>Present address: Petroleum Engineering Department, Cairo University, Giza, Egypt.

<sup>2</sup>Present address: Assistant Professor, Department of Petroleum Engineering, King Fahd University of Petroleum and Minerals, Dhahran 31261, Saudi Arabia; Petroleum Engineering Department, Cairo University, Giza, Egypt.

Contributed by the Petroleum Division of ASME for publication in the JOURNAL OF ENERGY RESOURCES TECHNOLOGY. Manuscript received May 28, 2015; final manuscript received April 5, 2016; published online May 5, 2016. Assoc. Editor: Gunnar Tamm.

and/or deflocculation. Oil skimming and gas removal from the waste water will help in minimizing the relative permeability damage effect. Biocides are usually used to stop the bacteria growth and keep the near wellbore area free of bacteria biomasses that severely affect the well injectivity. Also, other inhibitors and chemicals can be used to prevent scale formation, emulsification, precipitation of insoluble solids, and wax asphaltene deposition [9].

Based on field observation, it was concluded that a continuous loss of injectivity is obtained with matrix produced water reinjection [15], and successful PWRI is likely to require fracturing [16]. It is a commonly held belief within petroleum engineering that most successful water-injection wells have been fractured. When dealing with low permeability formations or with injection water of poor quality, fractures are usually induced intentionally in order to obtain a higher injectivity. Unintentional fracturing can also occur, for instance, when cold water is injected into a relatively hot reservoir. The cooling of the reservoir rock can reduce the rock stress to the point where the injection pressure exceeded the tensile strength of the rock and fracturing occurs [17,18].

**1.2 Skin Factor.** When the near wellbore region has a permeability that is higher or lower than the virgin rock permeability, the actual bottom-hole pressure will be different than the ideal bottom-hole pressure that would have been observed if the near wellbore region were untouched with the same properties as the virgin rock. This effect of having different permeabilities in the near wellbore and far wellbore region is called the skin effect. Skin factor is a dimensionless parameter that is used to quantify the magnitude of skin effect [19]. A positive skin factor is obtained when the near wellbore region has permeability lower than the native formation permeability (formation damage), while negative skin factor means the permeability of the near wellbore region has been increased (stimulation) [20].

Hawkins presented the following model to calculate the skin factor using the permeability and radius of the skin zone [21]

$$s = \left( \frac{k}{k_s} - 1 \right) \ln \left( \frac{r_s}{r_w} \right) \quad (1)$$

where  $k$  is the native formation permeability,  $k_s$  is the skin zone permeability,  $r_s$  is the skin zone radius,  $r_w$  is the wellbore radius, and  $s$  is the skin factor.

Injection of low quality water will damage the near wellbore region reducing its permeability and creating a positive skin factor. Hydraulic fracturing will enhance the well injectivity/productivity and will result in a negative skin factor.

The skin factor due to the presence of a hydraulic fracture can be calculated using the following equation [22]:

$$s = \ln \left[ \frac{r_w \left( \frac{\pi}{C_{fD}} + 2 \right)}{x_f} \right] \quad (2)$$

For a hydraulic fracture with infinite conductivity, Eq. (2) will take the following form:

$$s = \ln \left[ \frac{2r_w}{x_f} \right] \quad (3)$$

Equation (2) neglects the damage formed on the fracture faces. Mather et al. [23] developed a model to calculate the fracture skin taking in consideration the damage around the wellbore and fracture faces

$$s = \frac{\pi k}{2} \left[ \frac{r_s k_s k_{sd}}{(r_s - d)k_{sd} + dk_s} + \frac{(x_f - r_s)kk_d}{(r_s - d)k_d + dk_s} \right]^{-1} - \frac{\pi r_s}{2x_f} \quad (4)$$

Here,  $C_{fD}$  is the dimensionless fracture conductivity,  $d$  is the depth of the fracture face damage,  $k_d$  is the fracture face damage permeability,  $k_{sd}$  is the permeability in the region with near wellbore damage and fracture face damage, and  $x_f$  is the fracture half-length.

To apply Eq. (4) in actual field cases, fracture simulator will be needed to predict the fracture propagation rate with time at different injection flow rates. Also, lab work is needed to determine the damage parameters  $d$ ,  $k_d$ , and  $k_{sd}$ ; these parameters are strongly dependent on the properties of the solid content in the water (solid loading and particle size distribution) and on the pore throat size. For water disposal wells (especially commercial ones), water properties cannot be controlled since water comes from several sources. It is not practical to run for each water truck a complete water analysis to measure the solid contents, core analysis to define the damage parameters, and fracture simulator to predict the fracture propagation with time and flow rate.

Based on these facts, the development of a simple equation to predict the evolution of the skin factor with time is important in order to better predict the well behavior over long-term water injection. The developed equation idea is similar to the equation used for gas producer that states that the skin factor is linearly depend on the production flow rate. However, the problem that occurs during water injection is different than that observed during gas production since the skin factor in water injectors is time dependent as well as gas dependent. That said, running an SRT is all that is needed in order to develop and calibrate the new skin factor equation.

**1.3 Rate-Dependent Skin.** The term rate-dependent skin was originally used in association with high rate gas producing wells to describe the increase in skin factor at higher flow rates due to turbulent flow [24]

$$s' = s + Dq_g \quad (5)$$

Here,  $D$  is the non-Darcy coefficient,  $s'$  is the flow rate-dependent skin, and  $q_g$  is the gas flow rate.

In water-injection wells when injection is conducted through an unpropped hydraulic fracture, the fracture dimensions are different at different injection flow rates. A larger fracture will be developed at a higher flow rate to handle the larger water volume injected, and smaller fracture will be formed at lower injection flow rates. Based on Eqs. (3) and (4), the skin factor decreases with an increasing injection flow rate because of the longer fracture formed at higher injection rates.

Beside the injection flow rate effect, the fracture dimensions are function of time as well. At a constant injection flow rate, the fracture propagation continues with time until reaching a point where the fracture leak-off volume equals to the injection flow rate. After this point, the fracture will not propagate further unless the injected water damages the fracture faces which reduces leak-off and causes the fracture to propagate to handle the injected volumes. Usually, fracture propagation can be predicted by using a fracture simulation package [25,26]. However, geomechanical analysis is always needed to prepare the input data for the fracture simulators, which might consume time to prepare it.

The objective of this paper is to use injection test data to develop a simple equation to estimate the skin factor as a function of time and injection flow rate for a water injector well. A general form of the relationship is presented as well as a specific equation for a well in the Eagle Ford Shale basin in Texas, U.S.

## 2 Well Details

Data from a salt water disposal well located in Texas and used to dispose of produced water, flow back water, and drilling fluid water were analyzed in order to develop the targeted equation. The well is perforated through Escondido sands formation (Fig. 1).

The permeability of this formation was estimated to be very low (around 5 mD). Also, from the geomechanical analysis run using Advantek's @LOG software, the formation fracture pressure ranges between 2100 and 2450 psi (Fig. 2). Based on the permeability and fracture pressure value, successful injection requires the presence of a hydraulic fracture in this tight formation. The maximum allowable surface injection pressure (MASIP) for this well is between 1500 and 1600 psi.

Figure 3 shows the inflow and well performance curves. The curves show that under matrix injection and assuming no damage around the wellbore (skin=0), the maximum injection rate that could be achieved at MASIP is less than 0.5 bpm. To achieve injection flow rate higher than 4 bpm at MASIP, the formation should have a skin factor less than -6.5. From Eq. (3), the formation should have a hydraulic fracture with half-length more than 460 ft.

The well was treated using 120 bbls of 20% HCl at injection flow rate ranges from 2 bpm to 8 bpm. The well performance during the acid job is shown in Fig. 4. This figure shows the rate-dependent skin phenomenon due to the hydraulic fracture propagation: the skin factor at injection rate of 2 bpm was around -4, and at 8 bpm was less than -6.8. This reduction in the skin factor conforms to the interpretation of the development of increasing fracture length at higher injection flow rates.

### 3 Well Testing

Two injection tests (an SRT and pressure fall-off test (PFOT)) were conducted to evaluate the well performance and the fracture geometry. Figure 5 shows the pressure and rate data for the injection tests, while the injection schedule is given in Table 1.

Analyzing the SRT showed that for the three injection rates used in the test, the injection was always conducted under a hydraulic fracture flow regime. The three points on the pressure-rate plot lay on the same straight line (no change in the

slope), and the pressure was always higher than the minimum horizontal stress (MHS) value (Fig. 6) that has been calculated by using @LOG software as shown in Fig. 2.

Pressure fall-off data were analyzed to calculate the formation permeability and fracture dimensions. From the log-log diagnostic plot (Fig. 7), the different flow regimes were clearly identified: the early unity slope region identifies the wellbore storage interval; the fracture linear flow was identified by the half-slope line; the 3/2 slope line identifies the fracture closure; and finally, the pseudoradial flow region was identified by the zero slope line [27].

G-function is a time function that mainly used to estimate the closure time of fracture. This technique is dependent on fluid leak-off rate, and hence, it is considered as a preclosure analysis. The form of G-function used in this paper assumes high fluid efficiency in low permeability formation (which is true for water), and this validates the assumption of linear variation of fracture surface area with time during fracture propagation [28].

From the plot of G-function versus bottom-hole pressure and G-function versus its derivative (Fig. 8), the fracture closure pressure was identified to be 2480 psi. This value agrees with the value of MHS calculated from the well log using Advantek's @LOG software, which was 2450 psi. This result was expected as the closure pressure is equivalent to the MHS [29]. Summary of the fall-off test analysis is given in Table 2.

### 4 Development of the Rate-Dependent Skin Equation

The injection tests data were used to develop the new equation assuming that pseudoradial flow has been established. The skin factor for each flow rate was calculated using the following equation [30]:

$$BHP - P_i = \left[ \frac{70.6q\mu B}{kh} \right] \left[ \text{Ei} \left( \frac{-948\phi\mu c_r r_w^2}{kt} \right) + 2s \right] \quad (6)$$

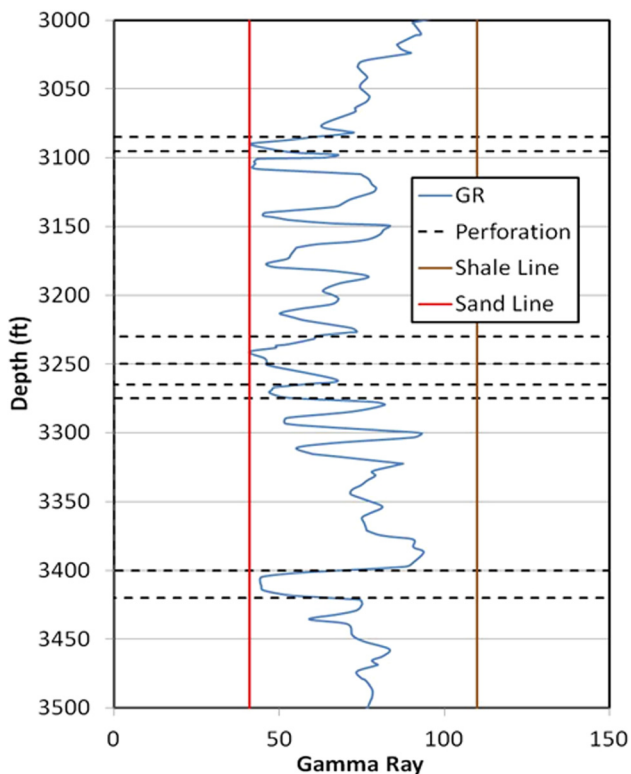


Fig. 1 The disposal well has four perforation intervals through Escondido formation (60 ft net perforations)

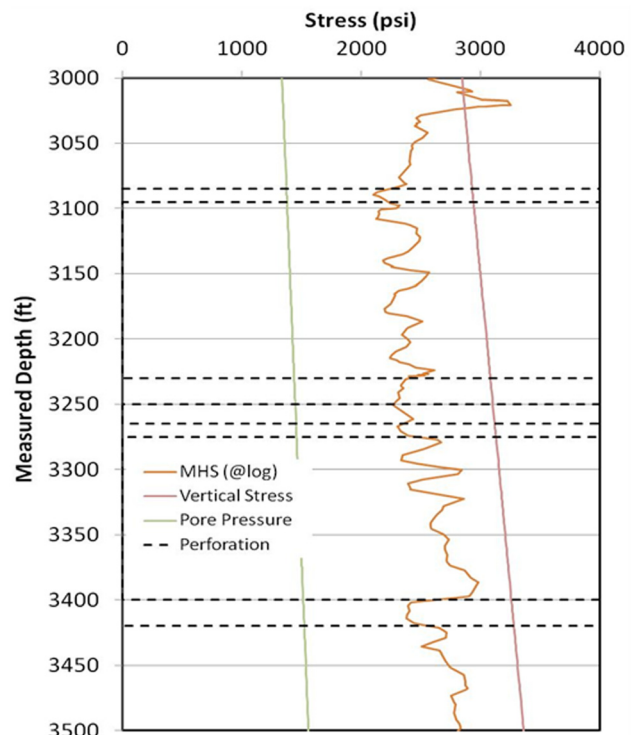


Fig. 2 Stress analysis of the Escondido formation

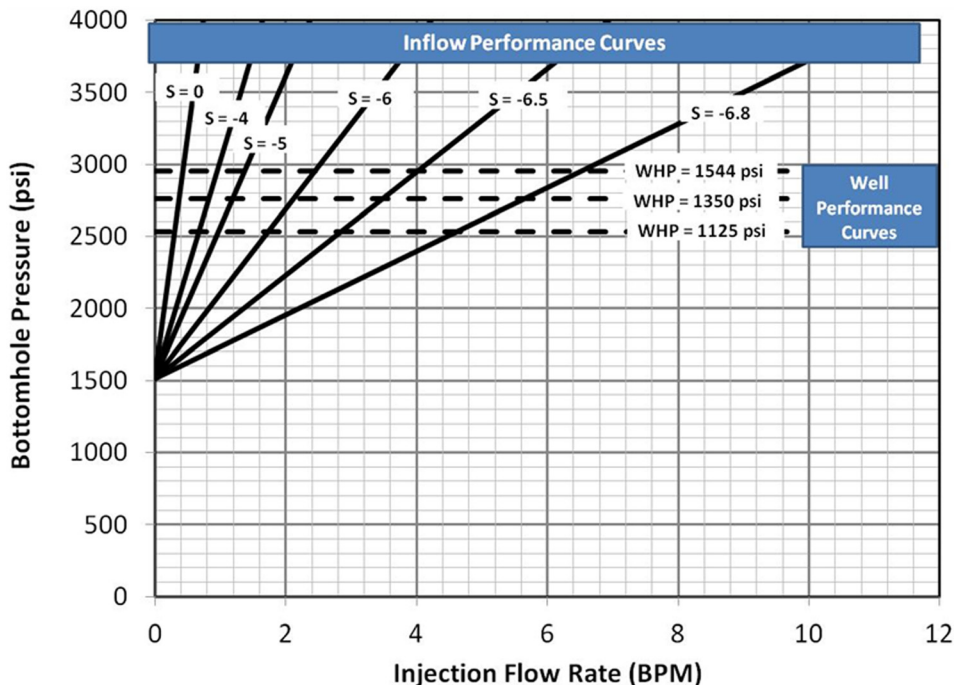


Fig. 3 Inflow and well performance curves

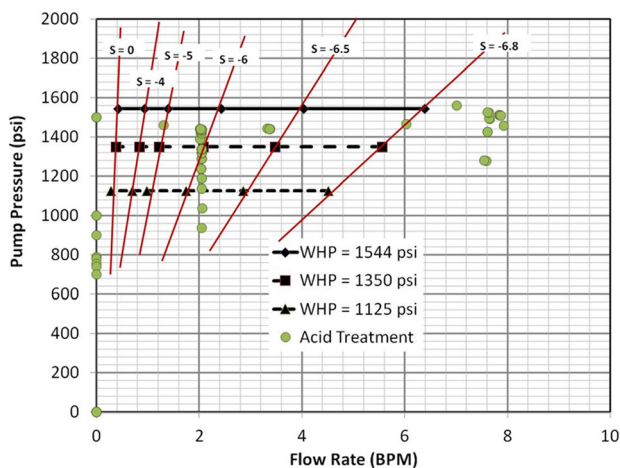


Fig. 4 Well performance during the well acidizing

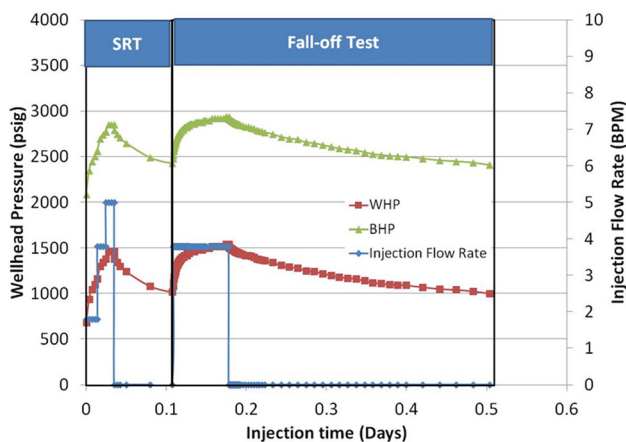


Fig. 5 Pressure and rate data for the SRT and PFOT

Solving Eq. (6) for skin factor yields

$$s = \frac{1}{2} \left( \frac{\text{BHP} - P_i}{\left[ \frac{70.6q\mu B}{kh} \right]} - \text{Ei} \left( \frac{-948\phi\mu c_t r_w^2}{kt} \right) \right) \quad (7)$$

Here,  $B$  is the formation volume factor, BHP is the bottom-hole pressure,  $c_t$  is the total compressibility,  $q$  is the injection flow rate,  $h$  is the formation thickness,  $P_i$  is the formation pressure (pore pressure),  $t$  is the injection duration,  $\phi$  is the formation porosity, and  $\mu$  is the fluid viscosity.

The skin factor was calculated at the end of each injection step, and the results obtained showed that the skin value decreased with increasing injection flow rate (Fig. 9). The following equation governs the change in the skin factor at different flow rates:

$$s = -0.3406 \left( \frac{q}{1440} \right) - 4.2999 \quad (8)$$

This equation can be generalized to be

$$s = a \left( \frac{q}{1440} \right) + b \quad (9)$$

where  $a$  and  $b$  are constants which depend on the well and fluid properties,  $s$  is the skin factor, and  $q$  is the injection flow rate in BPM.

The time factor is not considered in Eq. (9). This equation assumes that the fracture is developed to its maximum length at the time we start injecting, and it does not propagate after that. However, we know that the hydraulic fracture is propagating with time due to damage induced by the injection.

In order to include the injection time effect in the developed equation, the skin factor was calculated every 5 min of injection for each flow rate. Different skin development trends were noted for each flow rate as shown in Fig. 10. In general, a logarithmic relationship between the skin factor and injection time was captured and covered by the following equation:

$$s = -A \ln \left( \frac{t}{60} \right) - B \quad (10)$$

**Table 1 Injection tests schedule**

Injection duration (min)	Injection flow rate (BPM)	Volume injected (bbl)	Test
20	1.8	36	SRT
15	3.8	57	
15	5	75	
106	0	0	PFOT
100	3.8	380	
500	0	0	
Cumulative volume (bbl)		548	

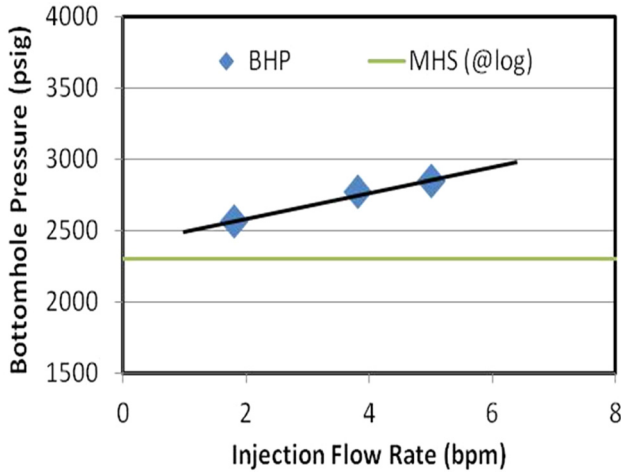


**Fig. 6 Pressure–rate plot (SRT analysis). MHS is the formation minimum horizontal stress.**

**Table 2 Fall-off test analysis results**

Parameter	Value
Permeability ( <i>k</i> ), mD	8.4
Transmissibility ( <i>kh/μ</i> ), mD ft/cP	508
Closure pressure ( <i>P<sub>c</sub></i> ), psi	2480
Closure time ( <i>t<sub>c</sub></i> ), hr	3.6

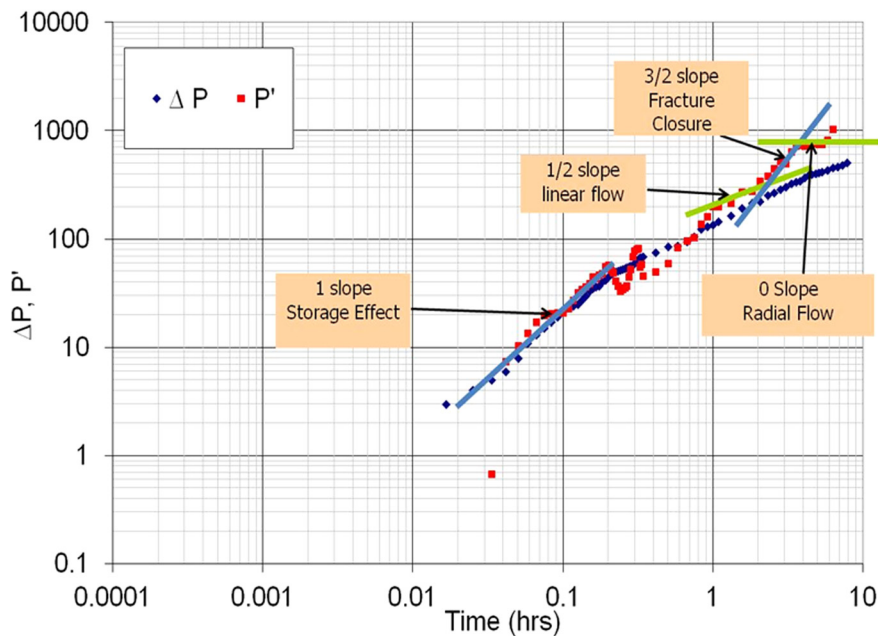


**Fig. 7 Log–log diagnostic plot for the water disposal well**

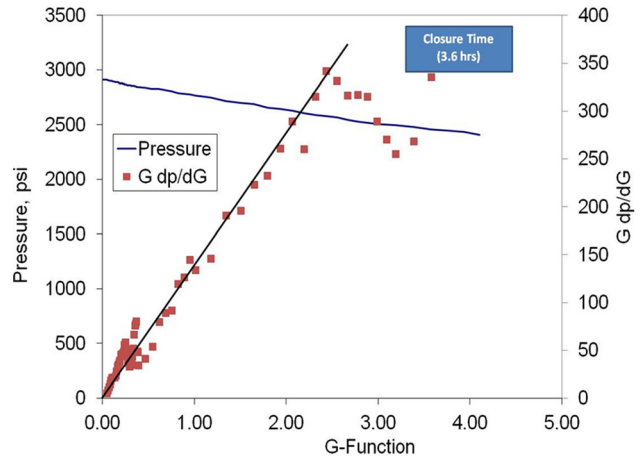


**Fig. 8 G-function analysis of the pressure fall-off data**

In the above equation, *A* and *B* are the fitting parameters and were controlled by the injection flow rate (Fig. 11) and can be calculated using the following equations:

$$A = Ce^{D(\frac{q}{1440})} \quad (11)$$

$$B = Ee^{F(\frac{q}{1440})} \quad (12)$$

where *C*, *D*, *E*, and *F* are the fitting parameters on the *A* and *B* versus *q* plots. They depend on the damage building rate, which is a function of the formation and fluid properties. The values of these constants for the current case are listed in Table 3.

The general rate-dependent skin equation for an unpropped hydraulically fractured injection well is as follows:

$$s = -Ce^{D(\frac{q}{1440})} \ln\left(\frac{t}{60}\right) - Ee^{F(\frac{q}{1440})} \quad (13)$$

The above equation can be developed for any injector by using the following steps:

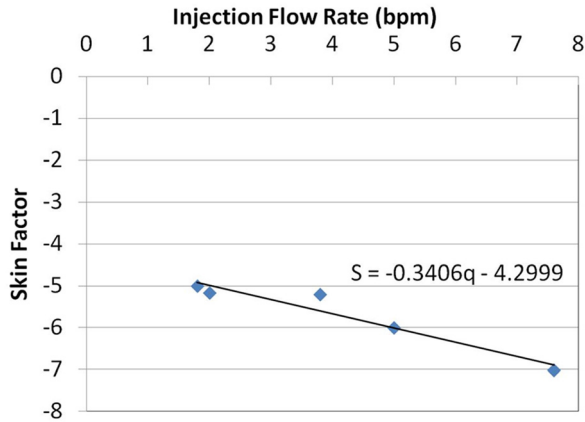


Fig. 9 The relationship between the skin factor and injection flow rate

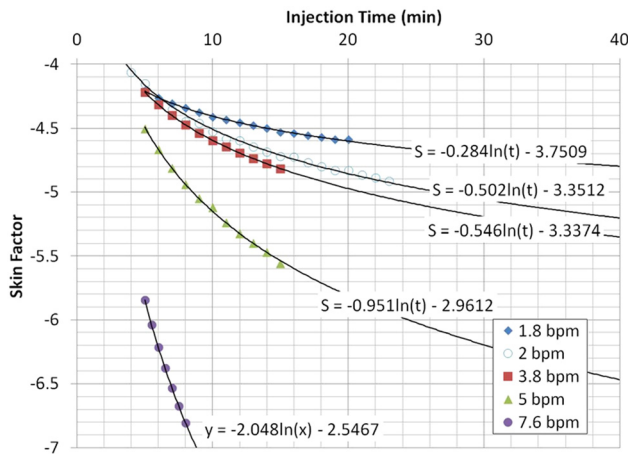


Fig. 10 The relationship between the skin factor and injection time

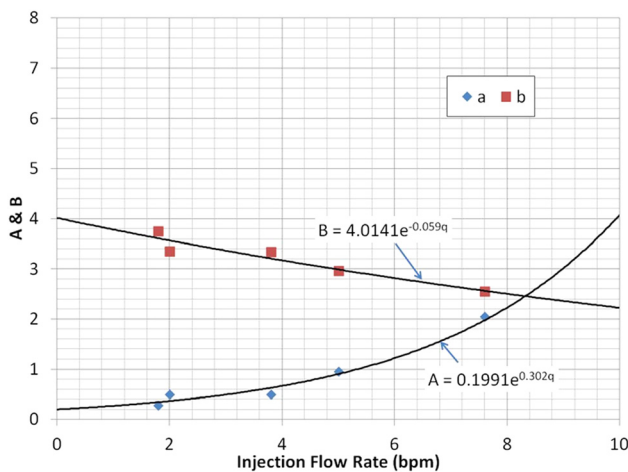


Fig. 11 The calculations of the C, D, E, and F constants

Table 3 Summary of the developed equation constants

Constant	C	D	E	F
Value	0.1991	0.302	4.0141	-0.059

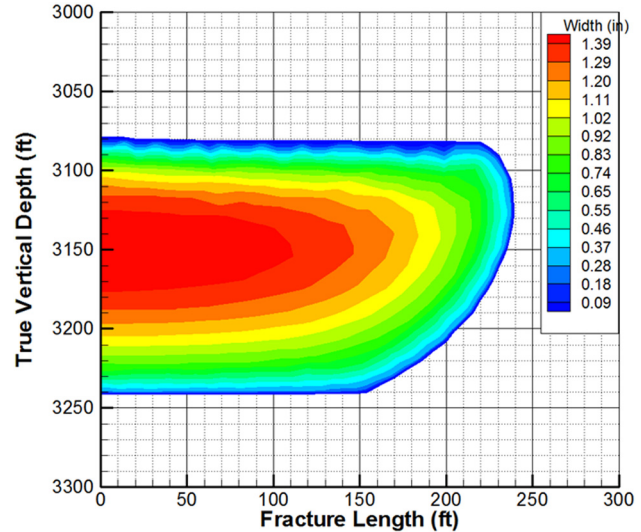


Fig. 12 Hydraulic fracture dimensions calculated by @FRAC3D

- (1) SRT should be conducted using the same fluid that will be used in the ongoing injection operations.
- (2) For each step, the skin factor to be calculated using Eq. (7) at multiple time steps.
- (3) For each flow, plot of skin factor versus injection time should be fitted to obtain the constants  $A$  and  $B$  in Eq. (10).
- (4) A relationship between  $A$ 's and  $B$ 's and the injection flow rate can be obtained as shown in Fig. 11.
- (5)  $C$  and  $D$  are the fitting parameters in the exponential relationship between  $A$  and  $q$  as shown in Fig. 11 and Eq. (11).
- (6)  $E$  and  $F$  are the fitting parameters in the exponential relationship between  $A$  and  $q$  as shown in Fig. 11 and Eq. (12).
- (7) Substitute  $A$  and  $B$  in Eq. (10) by Eqs. (11) and (12) to get the general skin expression (Eq. (13)).

## 5 Validations and Case Study

The PFOT data were used to check the validity of Eq. (13). The PFOT was conducted by injecting water at 3.8 bpm for 100 min. A 3D fracture simulation was conducted using Advantek's @FRAC3D simulator to monitor the fracture propagation. The simulator estimated fracture length of 239 ft at the end of the PFOT (Fig. 12). Using Eq. (3), the skin factor equivalent to this

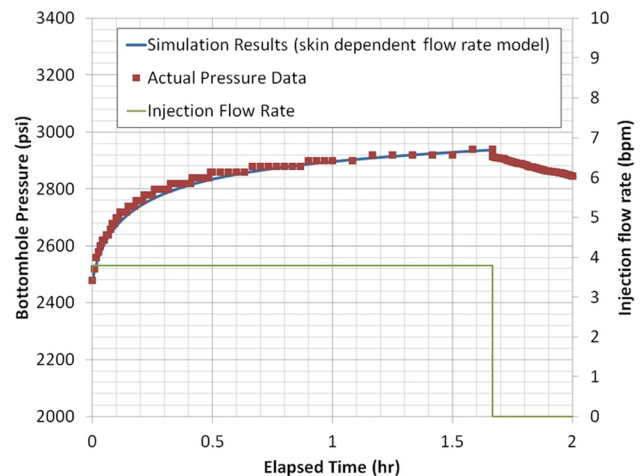


Fig. 13 A good match between the actual and calculated BHP was obtained for the PFOT

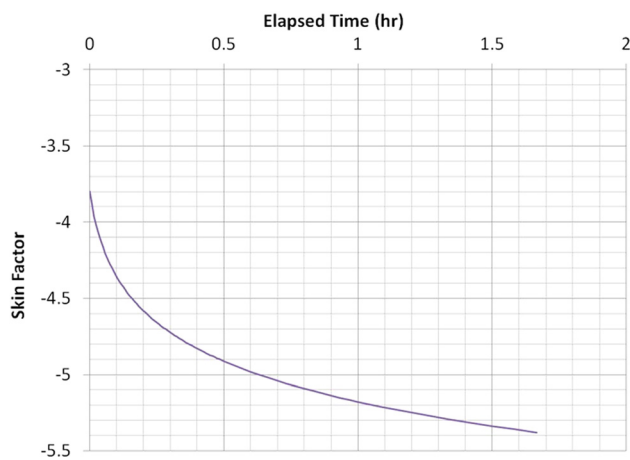


Fig. 14 Skin factor calculated using Eq. (13)

simulated fracture length is  $-5.82$ . The skin factor calculated from the field data at the end of the PFOT using the rate-dependent skin equation Eq. (13) is  $-5.9$ , which agrees very closely to the skin calculated from fracture simulator results.

The skin factor was calculated at several time steps, and using Eq. (6), the BHP was also calculated. A good match between the calculated and actual BHP during the PFOT was obtained as shown in Fig. 13. Using Eq. (13), the initial skin factor calculated to be  $-3.8$ , which indicates that the fracture opens up as soon as the injection initiated. As the fracture is propagating with time, the calculated skin is decreasing to reach  $-5.4$  after 1.8 hrs of injection as shown in Fig. 14.

The pressure is calculated assuming constant skin factor to highlight the significance of using the new model to predict the skin development and its impact on pressure calculations. Figure 15 shows that at high value skin factor (higher than  $-4$ ) which is

Table 4 Injection time and volume to reach MASIP

Injection flow rate (BPM)	Injection duration to reach MASIP (min)	Volume to be injected (bbl)
1	554	554
2	116	232
4	95	380
5	89	445
6	86	518

used in the calculations, the injection pressure was overestimated, and at low skin factor (less than  $-6$ ), the pressure was underestimated. However, when the average skin factor was used ( $-5$ ), the calculated pressure was initially less than the actual pressure, and after some time, the calculated pressure increased to be higher than the actual pressure. The match was only obtained when change in skin factor with time has been taken into consideration as shown in Fig. 14.

For the ongoing injection operations, the injection time before the pressure reaches the MASIP at each injection flow rate is shown in Table 4. The actual injection operation was conducted at 5 bpm, and the injection lasted for 87 min before the MASIP was reached, while the calculations showed that 89 min of injection would be accommodated at rate of 5 bpm before reaching the MASIP. This difference between the calculated time to reach MASIP and the actual time to reach MASIP of less than 2 min represents an error of less than 3%.

## 6 Conclusions

In this paper, a flow rate-dependent skin correlation was developed based on the data of and injection test from a water-injection well located in Texas, U.S. Based on the results of this study, the following conclusions can be drawn:

- (1) Using the developed equation can save the time and effort needed to use other complex formula and lab analysis that

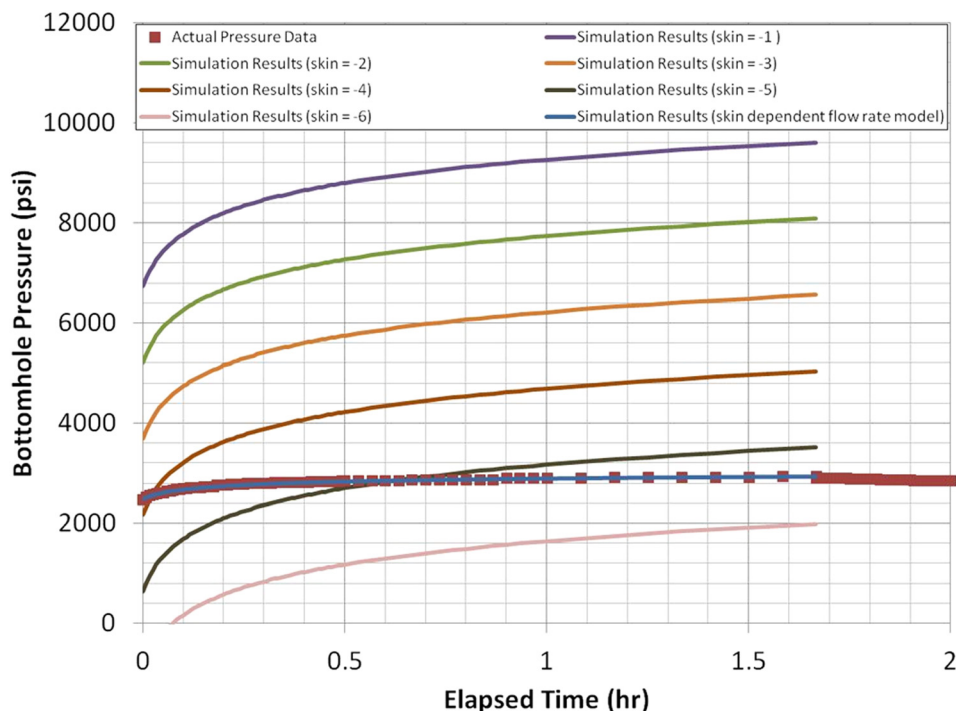


Fig. 15 Comparison between the injection pressures calculated using the skin-dependent flow rate model and constant skin values

is needed to obtain the damage parameters. To use the developed equation, all that is needed is an SRT using the water that will be used for ongoing injection.

- (2) A good match was obtained between the field data and the results obtained from the developed correlation. The development equation helped in predicting the ongoing injection operations with an error of less than 3%.
- (3) The constants shown in this paper are only valid to the injector well shown in this paper. To apply Eq. (13) generally, an injection test should be conducted first to calculate the constants  $E$ ,  $C$ ,  $D$ , and  $F$  as illustrated in this paper.
- (4) For water injection in an unpropped fracture, the skin factor depends on two factors: the injection flow rate and injection time.
- (5) The skin factor development rate is higher at higher injection rates (due to fracture propagation).

## Nomenclature

- $a$  and  $b$  = flow rate-dependent skin constants  
 $B$  = formation volume factor  
 BHP = bottom-hole pressure (psi)  
 $C$ ,  $D$ ,  $E$ , and  $F$  = time and Flow rate-dependent skin constants  
 $c_t$  = total compressibility (psi)<sup>-1</sup>  
 $c_{FD}$  = dimensionless fracture conductivity  
 $d$  = depth of the fracture face damage (ft)  
 $D$  = the non-Darcy coefficient (MSCF/d)<sup>-1</sup>  
 $h$  = formation thickness (ft)  
 $k$  = native formation permeability (mD)  
 $k_d$  = fracture face damage permeability (mD)  
 $k_s$  = skin zone permeability (mD)  
 $k_{sd}$  = permeability in the region with near wellbore damage and fracture face damage (mD)  
 $P_i$  = formation pressure (psi)  
 $q$  = injection flow rate (BPD)  
 $q_g$  = gas flow rate (MSCF/d)  
 $r_s$  = skin zone radius (ft)  
 $r_w$  = wellbore radius (ft)  
 $s$  = skin factor  
 $s'$  = flow rate-dependent skin  
 $t$  = injection time (hr)  
 $x_f$  = fracture half-length (ft)  
 $\mu$  = fluid viscosity (cP)  
 $\phi$  = formation porosity

## References

- [1] Roach, R. W., Carr, R. S., and Howard, C. L., 1993, "An Assessment of Produced Water Impacts at Two Sites in the Galveston Bay System," *Second State of the Bay Symposium*, Webster, TX, Feb. 4–6, Paper No. GBNEP 23.
- [2] Ali, M. A., Currie, P. K., and Salman, M. J., 2007, "Permeability Damage Due to Water Injection Containing Oil Droplets and Solid Particles at Residual Oil Saturation," *15th SPE Middle East Oil and Gas Show Conference*, Manama, Bahrain, Mar. 11–14, Paper No. SPE-104608-MS.
- [3] Technology Subgroup of the Operations and Environment Task Group, 2011, "Management of Produced Water from Oil and Gas Wells," NPC North America Resource Development Study, National Petroleum Council, Washington, DC, NPC, Report No. 2-17.
- [4] Clark, C. E., and Veil, J. A., 2009, "Produced Water Volumes and Management Practices in the United States," Environmental Science Division, Argonne National Laboratory for the U.S. Department of Energy, Office of Fossil Energy, National Energy Technology Laboratory, Washington, DC, Report No. ANL/EVS/R-09/1.
- [5] McCurdy, R., 2011, "Underground Injection Wells for Produced Water Disposal," Technical Workshops for the Hydraulic Fracturing Study: Water Resources Management, U.S. Environmental Protection Agency, Washington, DC, Paper No. EPA 600/R-11/048.
- [6] Diersing, N., 2009, *Water Quality: Frequently Asked Questions*, Florida Brooks National Marine Sanctuary, Key West, FL.
- [7] Patton, C. C., 1995, *Applied Water Technology*, 2nd ed., Campbell Petroleum Series, Norman, OK.
- [8] Pang, S., and Sharma, M. M., 1997, "A Model for Predicting Injectivity Decline in Water-Injection Wells," *SPE Form. Eval. J.*, **12**(3), pp. 194–201.
- [9] Bennion, D. B., Thomas, F. B., and Sheppard, D. A., 1992, "Formation Damage Due to Mineral Alteration and Wettability Changes During Hot Water and Steam Injection in Clay Bearing Sandstone Reservoirs," *SPE Formation Damage Control Symposium*, Lafayette, LA, Feb. 26–27, Paper No. SPE-23783-MS.
- [10] Dennis, M., and Turner, J., 1998, "Hydraulic Conductivity of Compacted Soil Treated With Biofilm," *J. Geotech. Geoenviron. Eng.*, **124**(2), pp. 120–127.
- [11] Bennion, D. B., Bennion, D. W., Thomas, F. B., and Bietz, R. F., 1998, "Injection Water Quality—A Key Factor to Successful Waterflooding," *J. Can. Pet. Technol.*, **37**(6), pp. 53–62.
- [12] Lei, W., Xiao-dong, W., Xu-min, D., Li, Z., and Chen, L., 2012, "Rate Decline Curves Analysis of a Vertical Fractured Well With Fracture Face Damage," *ASME J. Energy Resour. Technol.*, **134**(3), p. 032803.
- [13] Jin, L., and Wojtanowicz, A. K., 2014, "Development of Injectivity Damage Due to Oily Waste Water in Linear Flow," *SPE International Symposium and Exhibition on Formation Damage Control*, Lafayette, LA, Feb. 26–28, Paper No. SPE-168130-MS.
- [14] Rahman, M. K., Salim, M. M., and Rahman, M. M., 2012, "Analytical Modeling of Non-Darcy Flow-Induced Conductivity Damage in Propped Hydraulic Fractures," *ASME J. Energy Resour. Technol.*, **134**(4), p. 043101.
- [15] Detienne, J. L., Ochi, J., and Rivet, P., 2005, January 1, "A Simulator For Produced Water Re-injection in Thermally Fractured Wells," *SPE European Formation Damage Conference*, 25–27 May, Sheveningen, The Netherlands, May 25–27, Paper No. SPE-95021-MS.
- [16] van den Hoek, P. J., Al-Masfry, R. A., Zwarts, D., Jansen, J.-D., Hustedt, B., and Van Schijndel, L., 2009, "Optimizing Recovery for Waterflooding Under Dynamic Induced Fracturing Conditions," *SPE Reservoir Eval. Eng.*, **12**(5), p. SPE-110379-PA.
- [17] Perkins, T. K., and Gonzales, J. A., 1985, "The Effect of Thermoelastic Stress on Injection Well Fracturing," *SPE J.*, **25**(1), pp. 78–88.
- [18] Koning, E. J. L., and Niko, H., 1985, "Fractured Water-Injection Wells: A Pressure Falloff Test for Determining Fracture Dimensions," *SPE Annual Technical Conference and Exhibition*, Las Vegas, NV, Sept. 22–26, Paper No. SPE 14458.
- [19] Economides, M. J., Hill, A. D., and Ehlig-Economides, C., 1994, *Petroleum Production Systems*, Prentice Hall, Upper Saddle River, NJ.
- [20] Ahmed, T., and McKinney, P. D., 2005, *Advanced Reservoir Engineering*, Elsevier, Amsterdam, The Netherlands.
- [21] Hawkins, M. F., Jr., 1956, "A Note on the Skin Effect," *Trans. AIME*, **207**(1956), pp. 356–357.
- [22] Economides, M. J., Hill, A. D., Ehlig-Economides, C., and Zhu, D., 2012, *Petroleum Production Systems*, 2nd ed., Prentice Hall, Englewood Cliffs, NJ.
- [23] Mathur, A. K., Ning, X., Marcinew, R. B., Ehlig-Economides, C. A., and Economides, M. J., 1995, "Hydraulic Fracture Stimulation of Highly Permeability Formations: The Effect of Critical Fracture Parameters on Oilwell Production and Pressure," *SPE Annual Technical Conference and Exhibition*, Dallas, TX, Oct. 22–25, Paper No. SPE-30652-MS.
- [24] Cringarten, A. C., Ogunrewo, O., and Uxukbayev, G., 2012, "Assessment of Individual Skin Factors in Gas Condensate and Volatile Oil Wells," *SPE EUROPEC/EAGE Annual Conference and Exhibition*, Vienna, Austria, May 23–26, Paper No. SPE-143952-MS.
- [25] Salehi, S., and Nygaard, R., 2014, "Full Fluid–Solid Cohesive Finite-Element Model to Simulate Near Wellbore Fractures," *ASME J. Energy Resour. Technol.*, **137**(1), p. 012903.
- [26] Wang, W., and Dahi Taleghani, A., 2014, "Simulating Multizone Fracturing in Vertical Wells," *ASME J. Energy Resour. Technol.*, **136**(4), p. 042902.
- [27] Mohamed, I. M., Nasralla, R. A., Sayed, M. A., Marongiu-Porcu, M., and Ehlig-Economides, C. A., 2011, "Evaluation of After-Closure Analysis Techniques for Tight and Shale Gas Formations," *SPE Hydraulic Fracturing Technology Conference and Exhibition*, The Woodlands, TX, Jan. 24–26, Paper No. SPE-140136-MS.
- [28] Barree, R. D., Barree, V. L., and Craig, D. P., 2009, "Holistic Fracture Diagnostics: Consistent Interpretation of Prefrac Injection Test Using Multiple Analysis Methods," *SPE Prod. Oper.*, **24**(3), pp. 396–406.
- [29] DOE, 2004, "Evaluation of Impacts to Underground Sources of Drinking Water by Hydraulic Fracturing of Coalbed Methane Reservoirs," U.S. Department of Energy, Washington, DC, Report No. EPA 816-R-04-003.
- [30] Matthews, C. S., and Russell, D. G., 1967, *Pressure Buildup and Flow Tests in Wells* (Monograph Series), Society of Petroleum Engineers of AIME, Dallas, TX.